Nuclear Engineering and Technology 52 (2020) 654–659

Contents lists available at ScienceDirect

Nuclear Engineering and Technology

journal homepage: www.elsevier.com/locate/net

Original Article

Theoretical analysis on vibration characteristic of a flexible tube under the interaction of seismic load and hydrodynamic force

Jiang Lai*, [1], Chao He [1], Lei Sun, Pengzhou Li

Nuclear Power Institute of China, Chengdu, 610213, China

ARTICLE INFO

Article history:
Received 22 July 2019
Received in revised form
18 August 2019
Accepted 18 August 2019
Available online 23 August 2019

Keywords:
Flow-induced vibration
Flexible tube
Seismic load
Hydrodynamic force

ABSTRACT

The reliability of the spent fuel pool instrument is very important for the security of nuclear power plant, especially during the earthquake. The effect of the fluid force on the vibration characteristics of the flexible tube of the spent fuel pool instrument needs comprehensive analysis. In this paper, based on the potential flow theory, the hydrodynamic pressures acting on the flexible tube were obtained. A mathematical model of a flexible tube was constructed to obtain the dynamic response considering the effects of seismic load and fluid force, and a computer code was written. Based on the mathematical model and computer code, the maximum stresses of the flexible tube in both safe shutdown earthquake and operating basis earthquake events on the spent fuel pool with three typical water levels were calculated, respectively. The results show that the fluid force has an obvious effect on the stress and strain of the flexible tube in both safe shutdown earthquake and operating basis earthquake events.

1. Introduction

The spent fuel pools, which sit atop the reactor buildings and are meant to keep spent fuel submerged in water, are very important to the security of a nuclear power plant. During an earthquake, the mechanical characteristics of the spent fuel pools instrument would be more complicated under seismic load and fluid force. For a new designed spent fuel pool instrument, it is necessary to analyze the vibration responses of the elastic tube of the spent fuel pool instrument. Lots of structural aseismic analysis were performed in recent years. Jibson and Keefer [1] developed an approach for judging if a landslide or group of landslides of unknown origin was more likely to have formed as a result of earthquake shaking or in aseismic conditions. Sadek and Isam [2] presented a thorough study of the behavior of inclined micro-piles under seismic loading. Their studies provided valuable information about the influence of micro-piles inclined on dynamic amplification and on the seismic-induced internal forces in micro-piles. A new simplified pushover analysis procedure was proposed by Jan et al. [3], which could estimate the seismic demands of high-rise buildings. The dynamic characteristics of a commercial nuclear reactor internal structures under the action of seismic load were analyzed by Jhung and Hwang [4]. A seismic analysis of an entire nuclear power plant system was performed and the effects of the fluid on the dynamic behaviors of a liquid-metal fast-breeder reactor were also investigated by Koo and Lee [5]. Response spectrum analysis was carried out to investigate reactor vessel under design condition, normal operation condition and other service conditions based on a finite element model created by Ogino et al. [6], and the numerical results was validated with the experimental data. The seismic response analysis of reactor vessel structures and the primary coolant was carried out by Frano and Forasassi [7]. A 3D finite element model was set up to analyze the propagation of seismic waves as well as its derived structural effect. A mathematical model was presented by Kim and Jhung to determine an appropriate ground mass in a seismic response analysis [8]. Guan et al. [9] used ANSYS to complete the analysis of the behaviors of structures with and without wind generator, under EI-Centro earthquake wave and Taft earthquake wave. By comparing the results of those two models, the feasibility of the wind energy and building integration was verified. The seismic demand of a LFR with reference to European Lead System project considered one of the most promising innovative Generation IV reactor was evaluated by Frano and Forasassi [10]. The safety aspects of the ELSY reactor in the event of a safe shutdown earthquake were also analyzed. Penna et al. [11] presented a macro-element model specifically developed for simulating the cyclic in-plane response of masonry wall, with

* Corresponding author.
E-mail address: laijiang1983@163.com (J. Lai).
[1] These authors equally contributed to this work.

https://doi.org/10.1016/j.net.2019.08.012

possible applications in nonlinear static and dynamic analysis of masonry structures. A 3D finite element model of reactor coolant system was constructed by Tong et al. [12], and the seismic analysis was performed to obtain the stress and displacement response.

The spent fuel pool instrument consists of a flexible tube named measuring guide tube, which subjected to the action of fluid in the earthquake condition. So, the vibration characteristics of this flexible tube are very complicated. It is required to demonstrate that the flexible tube is adequately designed at the earthquake condition for the design life. In our previous studies, the flow-induced vibration of tube bundles subjected to two-phase flow has been investigated [13–15]. However, it is still a problem deserving further investigations for the effects of seismic load and hydrodynamic force on the vibration characteristics of a flexible tube. That is to say, what effects can the seismic load and hydrodynamic force have on the vibration displacement and stress of the tube? Theoretical study has to be performed on this problem because the problem considered in this study is a typical fluid-solid coupling problem. Under the interaction of seismic load and hydrodynamic force, the long flexible tube may appear great elastic deformation. Due to the large deformation, it could be very difficult to obtain the vibration characteristic of the tube by the finite element simulation. In this paper, a mathematical model of a flexible tube subjected to seismic load and hydrodynamic force was presented. A computer code based on the presented model was written. By using the mathematical model and computer code, the maximum stress and displacement of the flexible tube in both safe shutdown earthquake and operating basis earthquake events were calculated for different water level conditions.

2. Theoretical analysis

2.1. Theoretical model

The governing partial differential equation of a flexible tube of a spent fuel pool under the interaction of seismic load and fluid force, as shown in Fig. 1, can be expressed as:

$$EI\frac{\partial^4 u}{\partial z^4}+\frac{\rho A}{g}\frac{\partial^2}{\partial t^2}(u+u_g)-P=0 \tag{1}$$

where u is defined as the displacement of the flexible tube, E is the modulus of elasticity, I is the inertia moment of the flexible tube, ρ is the tube density, A is the cross area of the tube, u_g is the lateral displacement of the support induced by the earthquake which can be obtained from the seismic load spectra, P is the hydrodynamic force.

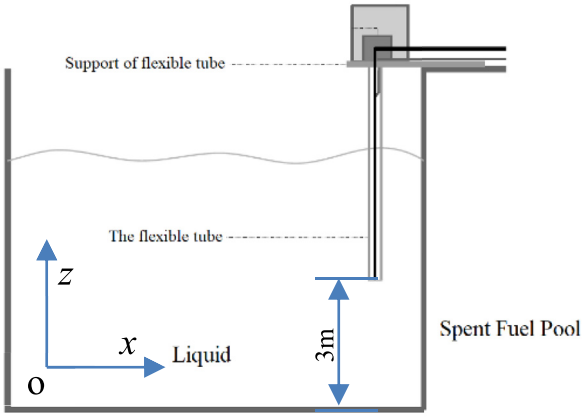

Fig. 1. Schematic diagram of a flexible tube of a spent fuel pool.

As shown in equation (1), the hydrodynamic force is an unknown quantity related to the displacement (including the elastic displacement of the tube), while the displacement is also affected by the hydrodynamic force. Therefore, this is a typical fluid-structure interaction problem. The hydrodynamic force analysis was presented in section 2.2, and the vibration analysis was presented in section 2.3.

2.2. Hydrodynamic force analysis

When seismic load is applied to the flexible tube, dynamic fluid pressure could be generated on both the inner and outer surface of the tube. It is reasonable to assume the disturbed fluid is a potential flow, which could satisfy Laplace's equation and potential theory. Thus, the three-dimensional Laplacian equation of the disturbed fluid can be expressed as [16]:

$$\frac{\partial^2\varphi}{\partial r^2}+\frac{1}{r}\frac{\partial\varphi}{\partial r}+\frac{1}{r^2}\frac{\partial^2\varphi}{\partial\theta^2}+\frac{\partial^2\varphi}{\partial z^2}=0 \tag{2}$$

where φ is the fluid velocity potential.

In order to reduce the complexity of the theoretical model, there are three reasonable assumptions as follows: (1) The fluid is an incompressible ideal fluid; (2) The fluid at the spent fuel pool bottom has no vertical velocity; (3) The fluid surface of the spent fuel pool is a free surface, and the effect of the free surface is neglected; (4) The vibration velocity of the flexible tube is the same as the fluid velocity; (5) The material of flexible tube is homogeneous, and the cross-sectional shape of the flexible tube does not change.

Thus, the boundary conditions can be expressed as:

$$z=0,\quad \frac{\partial\varphi}{\partial z}=0 \tag{3}$$

$$z=h,\quad \frac{\partial\varphi}{\partial t}=0 \tag{4}$$

$$r=a,\quad \frac{\partial\varphi}{\partial r}=\dot{u}_g\cos\theta+\frac{\partial u}{\partial t}\cos\theta \tag{5}$$

where $\dot{u}_g$ is the velocity of the support induced by the earthquake, $\partial u/\partial t$ is the velocity of elastic vibration of the flexible tube.

The velocity potential of the fluid in spent fuel pool can be expressed as:

$$\varphi(r,z,\theta,t)=\cos\theta\sum_{n=1}^{\infty}\dot{q}_n\sum_{s=1,3,5}^{\infty}f(r)\cos\frac{\pi s}{2h}z \tag{6}$$

where $f(r)$ is the function of cylindrical coordinate, $\dot{q}$ is the first derivative of generalized coordinates versus time which can be called as generalized velocity.

Substituting equation (6) into equation (1), the three-dimensional Laplacian equation can be rewritten as:

$$\frac{\partial^2 f(r_1)}{\partial r_1^2}+\frac{1}{r_1}\frac{\partial f(r_1)}{\partial r_1}-\left(1+\frac{1}{r_1^2}\right)f(r_1)=0$$
$$r_1=\frac{\pi s}{2h}\cdot r \tag{7}$$

The solution of equation (7) can be expressed as:

$$f(r_1) = B_{ns} I_{1s}(r_1) + C_{ns} K_{1s}(r_1) \tag{8}$$

where I_{1s} and K_{1s} are the modified Bessel functions of the first and second kinds, respectively, B_{ns} and C_{ns} are the constants determined by the boundary conditions.

The fluid acting on the flexible tube can be divided into the internal flow and external flow. The velocity potential of the internal flow of the flexible tube can be written as:

$$\varphi_1(r,z,\theta,t) = \cos \sum_{n=1}^{\infty} \dot{q}_n \sum_{s=1,3,5}^{\infty} B_{ns} I_{1s}(r_1) \cos \frac{\pi s}{2h} z \tag{9}$$

And the velocity potential of the external flow of the flexible tube can be written as:

$$\varphi_2(r,z,\theta,t) = \cos \sum_{n=1}^{\infty} \dot{q}_n \sum_{s=1,3,5}^{\infty} C_{ns} K_{1s}(r_1) \cos \frac{\pi s}{2h} z \tag{10}$$

As shown in equation (5), the first term is velocity of rigid motion, and the second term is the vibration velocity. Considering the two velocities separately, the boundary conditions for the internal flow can be expressed as:

$$\left.\frac{\partial \varphi_{1-rigid}}{\partial r}\right|_{r=a_2} = \dot{u}_g \cos\theta \tag{11}$$

$$\left.\frac{\partial \varphi_{1-elastic}}{\partial r}\right|_{r=a_2} = \frac{\partial u}{\partial t} \cos\theta \tag{12}$$

The boundary conditions for the external flow can be expressed as:

$$\left.\frac{\partial \varphi_{2-rigid}}{\partial r}\right|_{r=a_1} = \dot{u}_g \cos\theta \tag{13}$$

$$\left.\frac{\partial \varphi_{2-elastic}}{\partial r}\right|_{r=a_1} = \frac{\partial u}{\partial t} \cos\theta \tag{14}$$

where a_1 and a_2 is the outside and inside diameter of the flexible tube, respectively.

The hydrodynamic force acting on the flexible tube can be divided into two types of fluid force, one is the rigid body hydrodynamic force, another is the elastic vibrational hydrodynamic force.

For the rigid body hydrodynamic force, the velocity potentials of the internal and external flow can be expressed as:

$$\varphi_{1-rigid}(r,z,\theta,t) = \cos\theta \dot{u}_g \sum_{s=1,3,5}^{\infty} I_{1s}(r_1) B_s \cos \frac{\pi s}{2h} z \tag{15}$$

$$\varphi_{2-rigid}(r,z,\theta,t) = \cos\theta \dot{u}_g \sum_{s=1,3,5}^{\infty} K_{1s}(r_1) C_s \cos \frac{\pi s}{2h} z \tag{16}$$

Substituting equation (15) into equation (11), and equation (16) into equation (13), respectively, the undermined coefficient B_s and C_s can be obtained as:

$$\begin{aligned} B_s &= \frac{8h(-1)^{\frac{s-1}{2}}}{\pi^2 s^2 I'_{1s}(r_1)|_{r=a_2}} \\ C_s &= \frac{8h(-1)^{\frac{s-1}{2}}}{\pi^2 s^2 K'_{1s}(r_1)|_{r=a_1}} \end{aligned} \tag{17}$$

where h is the flexible tube length.

Then, the velocity potentials of the internal and external flow can be rewritten as:

$$\varphi_{1-rigid}(r,z,\theta,t) = \cos\theta \dot{u}_g \frac{8h}{\pi^2} \sum_{s=1,3,5}^{\infty} \frac{(-1)^{\frac{s-1}{2}} I_{1s}(r_1)}{s^2 I'_{1s}\left(\frac{\pi s}{2h} a_2\right)} \cos \frac{\pi s}{2h} z \tag{18}$$

$$\varphi_{2-rigid}(r,z,\theta,t) = \cos\theta \dot{u}_g \frac{8h}{\pi^2} \sum_{s=1,3,5}^{\infty} \frac{(-1)^{\frac{s-1}{2}} K_{1s}(r_1)}{s^2 K'_{1s}\left(\frac{\pi s}{2h} a_2\right)} \cos \frac{\pi s}{2h} z \tag{19}$$

The rigid body hydrodynamic forces of the internal and external flow can be expressed as:

$$\begin{aligned} P_{rigid-r=a_2} &= \frac{8h\gamma_0 a_2}{\pi g} \ddot{u}_g \sum_{s=1,3,5}^{\infty} \frac{(-1)^{\frac{s-1}{2}}}{s^2} \left[\frac{I_{1s}(r_1)}{I'_{1s}(r_1)}\right]\Big|_{r=a_2} \cos \frac{\pi s}{2h} z \\ P_{rigid-r=a_1} &= \frac{8h\gamma_0 a_1}{\pi g} \ddot{u}_g \sum_{s=1,3,5}^{\infty} \frac{(-1)^{\frac{s-1}{2}}}{s^2} \left[\frac{K_{1s}(r_1)}{K'_{1s}(r_1)}\right]\Big|_{r=a_1} \cos \frac{\pi s}{2h} z \end{aligned} \tag{20}$$

where $\ddot{u}_g$ is the maximum acceleration of the support induced by the earthquake, which can be obtained from the seismic load spectra.

So, the total rigid body hydrodynamic force can be expressed as:

$$\begin{aligned} P_{rigid} &= P_{rigid-r=a_2} + P_{rigid-r=a_1} \\ &= -\frac{8h\gamma_0}{\pi g} \ddot{u}_g \sum_{s=1,3,5}^{\infty} (-1)^{\frac{s-1}{2}} H_s \cos \frac{\pi s}{2h} z \end{aligned} \tag{21}$$

where,

$$H_s = \frac{1}{g^2} \left\{ a_1 \left[\frac{K_{1s}(r_1)}{K'_{1s}(r_1)}\right]\Big|_{r=a_1} + a_1 \left[\frac{I_{1s}(r_1)}{I'_{1s}(r_1)}\right]\Big|_{r=a_2} \right\} \tag{22}$$

For the elastic vibrational hydrodynamic force, the governing partial differential equation can be recast as a set of ordinary differential equations by Galerkin's method, with the eigenfunction q_n being used as a suitable set of base functions and X_n as the corresponding generalized coordinates.

$$u(z,t) = \sum_{n=1}^{\infty} q_n(t) X_n(z) \tag{23}$$

Substituting equations (6), (23) into equation (11), and equations (7), (23) into equation (12), respectively, the undermined coefficient B_{ns} and C_{ns} can be obtained as:

$$B_{ns} = \frac{4\int_0^h X_n \cos\frac{\pi s}{2h} z dz}{\pi s I_{1s}'\left(\frac{\pi s}{2h}a_2\right)}$$
$$C_{ns} = \frac{4\int_0^h X_n \cos\frac{\pi s}{2h} z dz}{\pi s K_{1s}'\left(\frac{\pi s}{2h}a_2\right)} \quad (24)$$

Then, the velocity potentials of the internal and external flow can be rewritten as:

$$P_{elastic} = P_{elastic-r=a_2} + P_{elastic-r=a_1} = -\frac{4\gamma_0}{g}\sum_{n=1}^{\infty}\ddot{q}_n \sum_{s=1,3,5}^{\infty} H_s \cdot s \cdot \cos\frac{\pi s}{2h} z \int_0^h X_n \cos\frac{\pi s}{2h}\xi d\xi d \quad (28)$$

2.3. Vibration analysis

Substituting the total rigid body and elastic vibrational hydrodynamic forces into equation (1), the vibration equations of the flexible tube can be rewritten as:

$$\sum_{n=1}^{\infty}\left[q_n\left(EI\frac{d^4X_n}{dz^4}\right) + \ddot{q}_n\left(\frac{\rho A}{g}X_n + \frac{4\gamma_0}{g}\sum_{s=1,3,5}^{\infty} H_s \cdot s \cdot \cos\frac{\pi s}{2h} z \int_0^h X_n \cos\frac{\pi s}{2h}\xi d\xi\right)\right] = -\ddot{u}_g\left[\frac{\rho A}{g} + \frac{8h\gamma_0}{\pi g}\sum_{s=1,3,5}^{\infty}(-1)^{\frac{s-1}{2}} H_s \cos\frac{\pi s}{2h} z\right] \quad (29)$$

$$\varphi_{1-elastic}(r,z,\theta,t) = \cos\theta\sum_{n=1}^{\infty}\dot{q}_n \sum_{s=1,3,5}^{\infty}\frac{I_{1s}(r_1)}{I_{1s}'\left(\frac{\pi s}{2h}a_2\right)}\frac{4}{\pi s} \times \cos\frac{\pi s}{2h} z \int_0^h X_n \cos\frac{\pi s}{2h}\xi d\xi \quad (25)$$

$$\varphi_{2-elastic}(r,z,\theta,t) = \cos\theta\dot{u}_g\sum_{n=1}^{\infty}\dot{q}_n \sum_{s=1,3,5}^{\infty}\frac{K_{1s}(r_1)}{K_{1s}'\left(\frac{\pi s}{2h}a_1\right)}\frac{4}{\pi s} \times \cos\frac{\pi s}{2h} z \int_0^h X_n \cos\frac{\pi s}{2h}\xi d\xi \quad (26)$$

The elastic vibrational hydrodynamic force of the internal and external flow can be expressed as:

$$P_{elastic-r=a_2} = -\frac{4\gamma_0 a_2}{g}\sum_{n=1}^{\infty}\ddot{q}_n \sum_{s=1,3,5}^{\infty}\left[\frac{I_{1s}(r_1)}{I_{1s}'(r_1)}\right]\Big|_{r=a_2}\frac{1}{s}\cos\frac{\pi s}{2h} z \int_0^h X_n \cos\frac{\pi s}{2h}\xi d\xi d$$
$$P_{elastic-r=a_1} = -\frac{4\gamma_0 a_1}{g}\sum_{n=1}^{\infty}\ddot{q}_n \sum_{s=1,3,5}^{\infty}\left[\frac{K_{1s}(r_1)}{K_{1s}'(r_1)}\right]\Big|_{r=a_1}\frac{1}{s}\cos\frac{\pi s}{2h} z \int_0^h X_n \cos\frac{\pi s}{2h}\xi d\xi d \quad (27)$$

So, the total elastic vibrational hydrodynamic force can be expressed as:

According to the orthogonality condition, the vibration equations can be rewritten as:

$$\ddot{q}_n + 2\varepsilon_n\dot{q}_n + \omega_n^2 q_n = -\eta_n\ddot{u}_g(t) \quad (30)$$

where

$$\eta_n = \frac{\int_0^h\left\{\frac{\rho A}{g}X_n + \frac{4\gamma_0}{g}X_n\sum_{s=1,3,5}^{\infty} H_s \cdot s\cos\frac{\pi s}{2h} z\int_0^h X_n\cos\frac{\pi s}{2h}\xi d\xi\right\}dz}{\int_0^h\left\{\frac{\rho A}{g}X_n^2 + \frac{4\gamma_0}{g}X_n\sum_{s=1,3,5}^{\infty} H_s \cdot s\frac{1}{s}\cos\frac{\pi s}{2h} z\int_0^h X_n\cos\frac{\pi s}{2h}\xi d\xi\right\}dz} \quad (31)$$

Comparing with the vibration equation of single degree of freedom under the action of seismic load,

$$\ddot{\delta}_n + 2\varepsilon_n\dot{\delta}_n + \omega_n^2\delta_n = -\ddot{u}_g(t) \quad (32)$$

$$q_n = \eta_n\delta_n \quad (33)$$

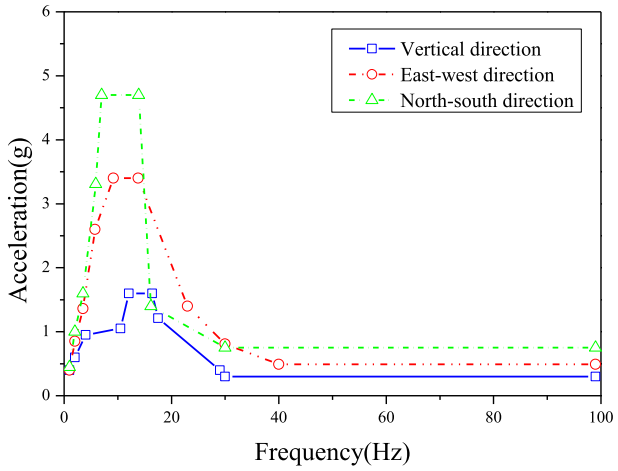

Fig. 2. The seismic load spectra at OBE event.

Finally, the displacement of the flexible tube under the action of seismic load and hydrodynamic force can be given as,

$$u(z,t) = \sum_{n=1}^{\infty} \sum_{r=1}^{\infty} A_{rn} X_{r(z)} \eta_n \delta_n \tag{34}$$

According to theory of elastic mechanics [17], based on the equilibrium equation, geometric equation, and physical equation, the stress of the flexible tube can be obtained.

3. Numerical results

Section 2 provides the analysis method of vibration characteristic of a flexible tube under the interaction of seismic load and hydrodynamic force. On the basis of the analyses above, the maximum stress and displacement of the flexible tube of a new designed spent fuel pool instrument are calculated in this section for two typical events of seismic analysis, respectively, which is called as safe shutdown earthquake (SSE) and operating basis earthquake (OBE). Safe shutdown earthquake is based on the estimated maximum potential earthquakes, taking into account reginal geological, seismic conditions and local subsurface soil properties. The ground motion caused by the safe shutdown earthquake is the largest. Under the action of this earthquake, the structures, systems and components of a nuclear power plant are required to maintain the original functions. And, the minimum peak ground acceleration (PGA) for OBE to be considered in design in certain regulations is related to the PGA for SSE. The seismic load spectra of OBE and SSE are illustrated in Fig. 2 and Fig. 3, respectively, which are the envelope spectra of seismic loads for Qinshan Nuclear Power Plant in China. As shown in Fig. 2, the maximum accelerations of the support induced by the earthquake in the vertical, east-west, and north-south directions are 1.6 g, 3.4 g, and 4.7 g at OBE event, respectively. As shown in Fig. 3, the maximum accelerations of the support induced by the earthquake in the vertical, east-west, and north-south directions are 2.4 g, 5.2 g, and 7.2 g at SSE event, respectively.

Table 1
The maximum stress of the flexible tube.

Depth of water	Maximum stress for OBE	Maximum stress for SSE
4 m	1.99 MPa	4.66 MPa
8 m	12.32 MPa	28.87 MPa
12 m	14.54 MPa	34.11 MPa

As shown in Fig. 1, one side of the measuring tube is fixed to the ground base, and the other side of the measuring tube is vertically inserted into the spent fuel pool. The depth of the spent fuel pool is 12 m. The length of the flexible tube is 9 m, the outer diameter of the tube is 21. 3 mm, and the inner diameter of the tube is 17.3 mm. The material of the measuring tube is 316L stainless steel, the modulus of elasticity E is 210 GPa. According to the geometric positions of the spent fuel pool and the flexible tube in Fig. 1, it can be obviously seen that when the water level of the spent fuel pool is less than 3 m, the measuring tube may not be affected by the fluid force. Thus, in order to analyze the influence of the water depth, the maximum stresses of the measuring tube were calculated at three water levels of the spent fuel pool considered in this study, which is 4 m, 8 m, and 12 m, respectively, for both OBE and SSE events.

Seismic analysis was performed for both OBE and SSE. The maximum stresses of the flexible tube for both OBE and SSE were illustrated in Table 1 and Fig. 4, respectively. The maximum stresses of the flexible tube in operating-basis earthquake event for the three water levels are 1.99 MPa, 12.32 MPa, and 14.54 MPa, respectively. And, the maximum stresses of the flexible tube in safe shutdown earthquake event for the three water levels are 4.66 MPa, 28.87 MPa, and 34.11 MPa, respectively. It is obvious that for the same earthquake event, the maximum stress of the flexible tube

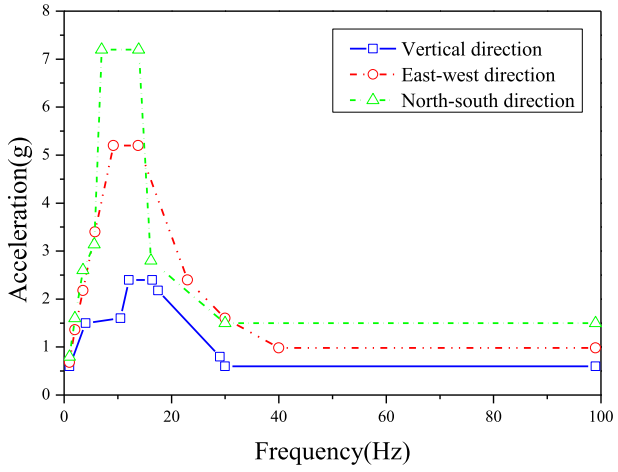

Fig. 3. The seismic load spectra at SSE event.

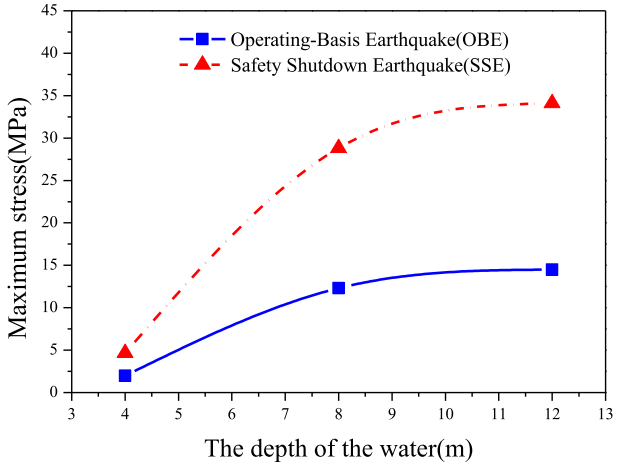

Fig. 4. The maximum stress of the flexible tube.

Table 2
The maximum displacement of the flexible tube.

Depth of water	Maximum displacement for OBE		Maximum displacement for SSE	
	North-south direction	East-west direction	North-south direction	East-west direction
4 m	0.38 mm	0.27 mm	0.88 mm	0.67 mm
8 m	3.59 mm	2.60 mm	8.28 mm	6.14 mm
12 m	10.75 mm	7.78 mm	24.61 mm	18.35 mm

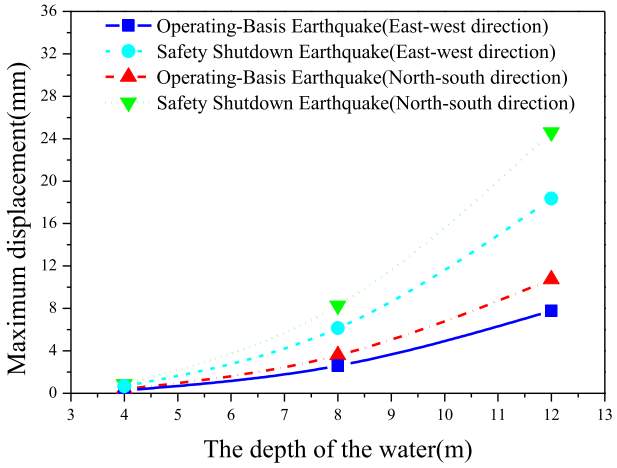

Fig. 5. The maximum displacement of the flexible tube in OBE and SSE events.

increases with the increasing depth of the water level of the spent fuel pool. For the example considered in this study, the maximum displacements in the north-south direction for SSE event incorporating the effect of fluid force are 0.88, 8.28, and 24.61 mm, which is 31.34%, 34.43%, and 34.11% more than the maximum displacements in the east-west direction. And, the maximum displacements in the north-south direction for OBE event incorporating the effect of fluid force are 0.38, 3.59, and 10.75 mm, which is 40.74%, 38.08%, and 38.17% more than the maximum displacements in the east-west direction. The numerical results of the maximum displacements of the flexible tube for the two events are illustrated in Table 2 and Fig. 5.

4. Conclusions

The dynamic characteristics of a flexible tube considering the effect of the seismic load and fluid force were investigated by building a mathematical model. Based on the potential flow theory, theoretical analysis was presented to obtain the rigid body hydrodynamic force induced by the rigid motion of the tube and the elastic vibrational hydrodynamic force induced by the elastic oscillation of the tube, respectively. Considering the effects of seismic loads and hydrodynamic forces, the dynamic responses of the flexible tube for SSE and OBE events were calculated. The results of calculations can be summarized as follows:

1. In the same earthquake event, the maximum stress and displacement of the flexible tube increases with the increasing depth of the water level of the spent fuel pool.
2. The maximum stresses and displacements of the flexible tube for the three water levels in SSE event are much greater than those in OBE event.
3. The maximum displacements of the flexible tube in the north-south direction for the three water levels are slightly larger than those in the east-west direction.
4. The analysis method presented in this study can be used to predict the vibration displacement and stress of a long flexible tube of a new designed spent fuel pool under the seismic load and hydrodynamic force for both SSE and OBE events.

Appendix A. Supplementary data

Supplementary data to this article can be found online at https://doi.org/10.1016/j.net.2019.08.012.

References

[1] R.W. Jibson, D.K. Keefer, Analysis of the seismic origin of landslides: examples from the New Madrid seismic zone, Geol. Soc. Am. Bull. 105 (4) (1993) 521–536.
[2] M. Sadek, S. Isam, Three-dimensional finite element analysis of the seismic behavior of inclined micro-piles, Soil Dyn. Earthq. Eng. 24 (6) (2004) 473–485.
[3] T.S. Jan, W.L. Ming, C.K. Ying, An upper-bound pushover analysis procedure for estimating the seismic demands of high-rise buildings, Eng. Struct. 26 (1) (2004) 117–128.
[4] M.J. Jhung, W.G. Hwang, Seismic response of reactor vessel internals for Korean standard nuclear power plant, Nucl. Eng. Des. 165 (1996) 57–66.
[5] G.H. Koo, J.H. Lee, Fluid effects on the core seismic behavior of a liquid metal reactor, J. Mech. Sci. Technol. 18 (12) (2004) 2126–2136.
[6] M. Ogino, R. Shioya, H. Kawai, S. Yoshimura, Seismic response analysis of nuclear pressure vessel model with adventure system on the earth simulator, J Earth Simulator 2 (2005) 41–54.
[7] R.L. Frano, G. Forasassi, Conceptual evaluation of fluid-structure interaction effects coupled to seismic event in an innovative liquid metal nuclear reactor, Nucl. Eng. Des. 239 (2009) 2333–2342.
[8] Y.W. Kim, M.J. Jhung, Mathematical analysis using two modeling techniques for dynamic responses of a structure subjected to a ground acceleration time history, Nucl. Eng. Technol. 43 (2011) 361–374.
[9] X.J. Guan, G.P. Chen, Y. Yang, Analyze of the seismic behavior of wind energy building, Adv. Mater. Res. 368 (2012) 934–937.
[10] R.L. Frano, G. Forasassi, Preliminary evaluation of the seismic response of the ELSYLFR, Nucl. Eng. Des. 242 (2012) 361–368.
[11] A. Penna, S. Lagomarsino, A. Galasco, A nonlinear macro-element model for the seismic analysis of masonry buildings, Earthq. Eng. Struct. Dyn. 43 (2) (2014) 159–179.
[12] L.L. Tong, R. Duan, X.W. Cao, Seismic analysis of RCS with finite element model for advanced PWR, Prog. Nucl. Energy 79 (2015) 142–149.
[13] J. Lai, L. Sun, P. Li, J. Yang, Z. Xi, C. He, Study on vortex-induced vibration of the tubes in a nuclear engineering test reactor, Nucl. Eng. Des. 330 (2018) 391–399.
[14] J. Lai, Analysis on streamwise fluidelastic instability of rotated triangular tube arrays subjected to two-phase flow, Mech. Syst. Signal Process. 123 (2019) 192–205.
[15] J. Lai, L. Sun, P. Li, T. Tan, L. Gao, Z. Xi, C. He, H. Liu, Eigenvalue analysis on fluidelastic instability of a rotated triangular tube array considering the effects of two-phase flow, J. Sound Vib. 429 (2019) 194–207.
[16] Guangjiong Zhou, Zongyi Yan, Shixiong Xu, Keben Zhang, Fluid Mechanics, Higher Education Press, Beijing, 2000.
[17] Zhilun Xu, Elastic Mechanics, Higher Education Press, Beijing, 2004.